Predicting and Correcting Scale Induced Biases Resulting from the Application of Regional Orbit and Clock Corrections

Lennard Huisman and Peter J.G. Teunissen

Abstract

Real-time orbit and clock corrections to GPS broadcast ephemeris, in short broadcast corrections (BCs), have become available as International GNSS Service (IGS) products through the IGS Real-time Service (RTS) in 2013. The BCs are distributed via the Network Transport of RTCM by Internet Protocol (NTRIP) according to RTCM State Space Representation standards. When applying the BCs in real-time Precise Point Positioning (PPP), user positions with sub-decimetre precision after convergence can be obtained. The IGS BCs refer to the International Terrestrial Reference Frame 2008 (ITRF2008). BCs in regional reference frames (RBCs) are available through regional NTRIP broadcasters in Europe, North-America, South-America and Australia.

The IGS RTS website states that: *Applying orbit and clock corrections from regional product streams in a real-time PPP solution automatically leads to regional coordinates. The PPP client would not need to transform coordinates because that is already done on the server side.* However, in contrast to the PPP-approach that uses BCs in ITRF2008 followed by a transformation to the local datum, the approach based on RBCs causes a bias in the PPP solution due to the scale factor between regional and global reference frames. This scale induced bias is satellite geometry dependent when the conventional 14-parameter transformation from the global to the regional reference frame is applied to the satellite position vectors in ITRF2008, to derive the RBCs from the IGS BCs. The size of the scale induced bias is significant. The bias is up to 8 cm for the Australian GDA94 and up to 0.5 cm for the North American NAD83.

Currently an additional satellite position dependent value is added to the satellite clock correction to deal with the scale induced biases of three RBCs, resulting in a transformed

L. Huisman (✉)
Kadaster, Apeldoorn, The Netherlands

Delft University of Technology, Delft, The Netherlands
e-mail: lennard.huisman@kadaster.nl

P.J.G. Teunissen
Curtin University, Bentley, WA, Australia

Delft University of Technology, Delft, The Netherlands
e-mail: p.teunissen@curtin.edu.au

International Association of Geodesy Symposia,
DOI 10.1007/1345_2015_117,

clock correction (Weber, BKG Ntrip Client (BNC) Version 2.9 – Manual, 2013). Applying these transformed clocks results in a remaining scale induced bias of less then 10 mm for each RBC of ETRF2000, NAD83 and SIRGAS2000. For GDA94 the remaining scale induced bias is maximum 30 mm, this is caused by the large scale factor of GDA94 compared to other regional reference frames.

This contribution will show that the remaining bias in the PPP solution is practically independent from satellite geometry and depends mainly on the user position; hence the remaining bias can be predicted and corrected for at any location.

Keywords
Global and regional broadcast corrections • Global and regional reference frames • Real-time precise point positioning

1 Introduction

Before real-time orbit and clock corrections to broadcast ephemeris, the so-called broadcast corrections (BCs), became available, Precise Point Positioning (PPP) has been a technique that was mainly used in post-processing (Kouba 2009). Products of the International GNSS Service (IGS), such as orbits and clocks, are made available in the IGS realization of the International Terrestrial Reference Frame (ITRF), currently IGS08, which is aligned to ITRF2008 (Rebischung et al. 2012).

Users however, are often interested in positions in a Regional Reference Frame (RRF) such as ETRF2000, NAD83, GDA94, SIRGAS2000 or SIRGAS95 . The rigorous approach to obtain a position in the RRF is to first compute the PPP solution in the Global Reference Frame (GRF) and then to transform this solution, obtained using IGS products, to the required RRF. With the aim to have the PPP solution directly refer to a RRF, an alternative approach, based on transforming the input IGS products to RRFs, was suggested in Kouba (2002).

The BCs that are made available through the IGS Real-Time Service are available in IGS08 and made available through NTRIP (Caissy et al. 2012; IGS 2013). They are referred to as the Global BCs (GBCs). Next to these GBCs there are RRF-referenced Regional BCs available from regional NTRIP-casters (BKG 2013a; IGS 2013). Transforming IGS satellite position products to RRFs leads to a location and geometry dependent bias between the PPP solution obtained using the rigorous approach and the approach using RBCs (Huisman et al. 2012; Teunissen et al. 2012). The source of this bias lies in the scale difference between the GRF IGS08 and the RRFs.

Several approaches, such as the unscaled and scale-absorbed approach, have been proposed to overcome this bias. Currently, the available RBCs are based on the transformed clocks approach, which adds a satellite dependent value to the real-time clock correction, to take out the scale induced bias for a reference position in the validity area of the RRF. The assumption is that this satellite dependent correction will decrease the size of the scale induced bias within the whole region of the RRF.

This contribution will first describe the rigorous approach for obtaining a position using PPP with GBCs. Next, the scale induced bias caused by the RBCs will be identified in Sect. 3. Section 4 introduces the unscaled, the scale-absorbed and the transformed clocks approach and will show that the remaining scale-induced bias of the unscaled and scale-absorbed approach can be easily computed for any location and any epoch (present, past and future).

We also show that the remaining scale-induced bias of the transformed clocks approach can be approximated very well by that of the easily computable scale-absorbed approach. This is demonstrated in Sect. 5 by means of experimental results of the transformed clocks approach. Section 6 summarizes the findings on the theoretical and practical aspects of the transformed clocks.

2 Obtaining a Position in the RRF with GBCs

GBCs give corrections to broadcast ephemeris such that precise satellite positions and clock information can be obtained. On the server side precise satellite positions and clock offsets are estimated/predicted using data from a global network of GNSS-receivers (Hauschild and Montenbruck 2009). The difference between satellite positions and clock offset from broadcast ephemeris and the real-time process on the server side is sent to users via NTRIP (Weber et al. 2005; RTCM 2011). Broadcast ephemeris data is available on the user side as this information is transmitted by the GNSS-satellites. A user adds the received GBC information to the satellite positions and clock offsets computed

from broadcast ephemeris to obtain the precise positions and clock offsets from the server side. The GBCs can be used in the PPP algorithm to obtain precise results in real-time, for example with software such as the BKG NTRIP Client (BNC) (Weber 2013) and RTKLIB (Takasu 2010). A GRF-to-RRF coordinate transformation is then finally applied to obtain the receiver antenna position in the required RRF.

The GRF-to-RRF transformation is time-dependent so as to take various dynamics (e.g. tectonic movements) into account. For a specific epoch t, the 14-parameter GRF-to-RRF transformation reduces to a 7-parameter similarity transformation:

$$\mathbf{x}_R(t) = \mathbf{d}(t) + s(t)\mathbf{R}(t)\mathbf{x}_G(t) \tag{1}$$

where

$$\mathbf{d}(t) = \begin{bmatrix} d_x(t) \\ d_y(t) \\ d_z(t) \end{bmatrix}$$

$$s(t) = (1 + \Delta s(t))$$

$$\mathbf{R}(t) = \begin{bmatrix} 1 & -r_z(t) & r_y(t) \\ r_z(t) & 1 & -r_x(t) \\ -r_y(t) & r_x(t) & 1 \end{bmatrix}$$

with

$\mathbf{x}_G$: Coordinate vector in the global frame (GRF) x_G, y_G, z_G
$\mathbf{x}_R$: Coordinate vector in the regional frame (RRF) x_R, y_R, z_R
$\mathbf{d}$: Vector with translation parameters d_x, d_y, d_z
s : Scale factor between GRF and RRF
Δs : Increment of s to 1
$\mathbf{R}$: Matrix with differential rotation angles r_x, r_y, r_z

The transformation parameters are often considered to be dependent on time, in which case their time dependency needs to be known as well. Usually it is sufficient to only consider their linear time dependency. In that case the transformation is referred to as a 14-parameter transformation. The 14 parameters then consist of the 7 similarity transformation parameters, plus their 7 time-rates of change, all given at a certain reference epoch t_0. These 14 parameters can then be used to compute the 7 similarity transformation parameters for any epoch t as

$$\begin{aligned} \mathbf{d}(t) &= \mathbf{d}(t_0) + (t - t_0)\dot{\mathbf{d}}(t_0) \\ \mathbf{R}(t) &= \mathbf{R}(t_0) + (t - t_0)\dot{\mathbf{R}}(t_0) \\ \Delta s(t) &= \Delta s(t_0) + (t - t_0)\Delta\dot{s}(t_0) \end{aligned} \tag{2}$$

with

$\dot{\mathbf{d}}$: Rate of change of the translation vector
$\dot{\mathbf{R}}$: Rate of change of the rotation matrix
$\dot{\Delta s}$: Rate of change of the scale factor

3 The RBC Approach with Scale Induced Bias

In the RBC approach the GRF-to-RRF transformation is applied on the server side to the satellite positions. When a user applies the RBCs to the satellite positions from broadcast ephemeris the resulting positions are in the RRF. The RRF does not have the same scale as the observations, which is the case for the GRF. The receiver-to-satellite range, in a GRF, is computed as:

$$\rho^s_{r,G} = ||\mathbf{x}^s_G - \mathbf{x}_{r,G}|| \tag{3}$$

Substituting Eq. (1) into Eq. (3), taking the invariance of the norm with relation to the rotations into account, gives

$$\rho^s_{r,G} = \frac{1}{1 + \Delta s}||\mathbf{x}^s_R - \mathbf{x}_{r,R}|| = \frac{1}{1 + \Delta s}\rho^s_{r,R} \tag{4}$$

With

$$\frac{1}{1 + \Delta s} = 1 - \frac{\Delta s}{1 + \Delta s}$$

we may write

$$\begin{aligned} \rho^s_{r,G} &= ||\mathbf{x}^s_G - \mathbf{x}_{r,G}|| \\ &= ||\mathbf{x}^s_R - \mathbf{x}_{r,R}|| - \tfrac{\Delta s}{1+\Delta s}||\mathbf{x}^s_R - \mathbf{x}_{r,R}|| \\ &= ||\mathbf{x}^s_R - \mathbf{x}_{r,R}|| - \Delta s||\mathbf{x}^s_G - \mathbf{x}_{r,G}|| + \tfrac{\Delta s^2}{1+\Delta s} \\ &\quad ||\mathbf{x}^s_G - \mathbf{x}_{r,G}|| \\ &\approx ||\mathbf{x}^s_R - \mathbf{x}_{r,R}|| - \Delta s||\mathbf{x}^s_G - \mathbf{x}_{r,G}|| \\ &\approx \rho^s_{r,R} - \Delta s||\mathbf{x}^s_G - \mathbf{x}_{r,G}|| \end{aligned} \tag{5}$$

The size of $\frac{\Delta s^2}{1+\Delta s}||\mathbf{x}^s_G - \mathbf{x}_{r,G}||$ is at the micrometer level for currently existing RRFs and can therefore be ignored in Eq. (5). The presence of the last term in the above equation, $\Delta s||\mathbf{x}^s_G - \mathbf{x}_{r,G}||$, is the cause of the scale induced bias in the RBC approach. It has the following effect on the (simplified) observation equation,

$$\begin{aligned} p^s_r &= \rho^s_{r,G} + cdt_r - cdt^s + a^s_r + e^s_r \\ &= \rho^s_{r,R} - \Delta s||\mathbf{x}^s_G - \mathbf{x}_{r,G}|| + cdt_r - cdt^s + a^s_r + e^s_r \end{aligned} \tag{6}$$

with p^s_r the observation, cdt_r and cdt^s the receiver and satellite clock offsets in meters, a^s_r the atmospheric propagation delay and e^s_r denoting unmodelled errors and measurement

noise. As the scale induced bias is not parametrized in the PPP model, the bias $\Delta s||\mathbf{x}^s_G - \mathbf{x}_{r,G}||$ will be absorbed by the parameters which are solved for in the PPP algorithm, $\mathbf{x}_{r,R}$ and cdt_r.

4 Methods to Deal with the Scale Induced Bias

In the following three sections, methods are presented that deal with the scale induced bias, without the need of having to change the positioning algorithm. The residual biases of the three methods will also be described.

4.1 The Unscaled Approach

In the unscaled approach the scale induced bias is eliminated by ignoring the increment to scale. The applied transformation in the 'unscaled' case becomes

$$\mathbf{x}_{R'} = \mathbf{d} + \mathbf{R}\mathbf{x}_G \tag{7}$$

The relation between R- and unscaled R'-frame is (cf. Eq. (1)):

$$\mathbf{x}_R = \mathbf{x}_{R'} + \Delta s\ \mathbf{R}\ \mathbf{x}_G \tag{8}$$

Application of the unscaled transformation gives

$$\rho^s_{r,G} = ||\mathbf{x}^s_G - \mathbf{x}_{r,G}|| = ||\mathbf{x}^s_{R'} - \mathbf{x}_{r,R'}|| = \rho^s_{r,R} \tag{9}$$

and Eq. (6) becomes

$$p^s_r = \rho^s_{r,R'} + cdt_r - cdt^s + a^s_r + e^s_r \tag{10}$$

When using this observation equation, one solves the user position vector as $\mathbf{x}_{r,R'}$, implying that one is left with the following residual bias for the unscaled approach,

$$\begin{aligned} \mathbf{b}^{us}_r &= \mathbf{x}_{r,R'} - \mathbf{x}_{r,R} = -\Delta s\ \mathbf{R}\ \mathbf{x}_{r,G} \\ ||\mathbf{b}^{us}_r|| &= \Delta s||\mathbf{x}_{r,G}|| \end{aligned} \tag{11}$$

As shown in Huisman et al. (2012) and Teunissen et al. (2012), this remaining bias in the unscaled approach can be ignored for the horizontal component. Its vertical component is constant over large areas. In other words the remaining bias in the unscaled approach is location independent for practical purposes and only affects height.

4.2 The Scale-Absorbed Approach

As in the unscaled approach, the scale induced bias is eliminated by ignoring the increment to scale in the scale-absorbed approach. Additionally the bias of the unscaled approach, given in Eq. (11), is accounted for by adding this bias for a reference point to the translation vector. The applied transformation in the 'scale absorbed' case becomes:

$$\mathbf{x}_{R''} = \mathbf{d}' + \mathbf{R}\mathbf{x}_G \quad \text{with } \mathbf{d}' = \mathbf{d} + \Delta s\mathbf{R}\mathbf{x}_{*,G} \tag{12}$$

with $\mathbf{x}_{*,G}$ being the coordinate vector of a reference-point. The relation between R- and scale-absorbed R''-frame is (cf. Eq. (1)):

$$\mathbf{x}_R = \mathbf{x}_{R''} + \Delta s\ \mathbf{R}\ (\mathbf{x}_G - \mathbf{x}_{*,G}) \tag{13}$$

Application of the scale-absorbed transformation gives

$$\rho^s_{r,G} = ||\mathbf{x}^s_G - \mathbf{x}_{r,G}|| = ||\mathbf{x}^s_{R''} - \mathbf{x}_{r,R''}|| = \rho^s_{r,R''} \tag{14}$$

and

$$p^s_r = \rho^s_{r,R''} + cdt_r - cdt^s + a^s_r + e^s_r \tag{15}$$

with the bias of $\mathbf{x}_{r,R''}$, which is solved for in the scale-absorbed (sa) approach, following from (13) as

$$\begin{aligned} \mathbf{b}^{sa}_r &= \mathbf{x}_{r,R''} - \mathbf{x}_{r,R} = -\Delta s\ \mathbf{R}\ (\mathbf{x}_{r,G} - \mathbf{x}_{*,G}) \\ ||\mathbf{b}^{sa}_r|| &= \Delta s||\mathbf{x}_{r,G} - \mathbf{x}_{*,G}|| \end{aligned} \tag{16}$$

When $\mathbf{x}_{*,G}$ is chosen such that $||\mathbf{x}_{r,G} - \mathbf{x}_{*,G}|| < ||\mathbf{x}_{r,G}||$ for the region in which the RRF is valid, this bias is of course smaller than for the unscaled approach.

4.3 The Transformed Clocks Approach

In the transformed clocks approach the scale induced bias is accounted for by adding the scale induced effect of Eq. (5) to the satellite clock error, thus resulting in a transformed clock,

$$\widetilde{cdt}^s_R = cdt^s + \Delta s||\mathbf{x}^s_G - \mathbf{x}_{*,G}|| \tag{17}$$

To show the effect of $\widetilde{cdt}^s_R$ on the receiver position obtained using the PPP algorithm, first define

$$\tilde{\mathbf{x}}_{r,R} = \mathbf{x}_{r,R} - \Delta\mathbf{x}_R \quad \text{with } \Delta\mathbf{x}_R = \Delta s\mathbf{R}(\mathbf{x}_{r,G} - \mathbf{x}_{*,G}) \tag{18}$$

Then we have to first order (i.e. after linearisation):

$$\begin{aligned} ||\mathbf{x}^s_R - \tilde{\mathbf{x}}_{r,R}|| &= ||\mathbf{x}^s_R - \mathbf{x}_{r,R} + \Delta\mathbf{x}_R|| \\ &\approx ||\mathbf{x}^s_R - \mathbf{x}_{r,R}|| + (\mathbf{u}^s_{r,R})^T\Delta\mathbf{x}_R \\ &\approx ||\mathbf{x}^s_R - \mathbf{x}_{r,R}|| + \Delta s(\mathbf{u}^s_{r,G})^T(\mathbf{x}_{r,G} - \mathbf{x}_{*,G}) \end{aligned} \tag{19}$$

and

$$||\mathbf{x}^s_G - \mathbf{x}_{*,G}|| \approx ||\mathbf{x}^s_G - \mathbf{x}_{r,G}|| + (\mathbf{u}^s_{r,G})^T(\mathbf{x}_{r,G} - \mathbf{x}_{*,G}) \tag{20}$$

Table 1 Range of the predicted remaining scale induced bias for RBCs at August 9th 2013

RRF	Translation parameters d_x,d_y,d_z (mm)	Scale increment Δs (10^{-9})	Rotation angles r_x,r_y,r_z (mas)	Reference point $x_{*,G},y_{*,G},z_{*,G}$ (m)	Predicted bias maximum $\|\|\mathbf{b}_r^{tc}\|\|$ (mm)
NAD83	1004.6		−27.02	−1092950.0	
	−1912.4	−0.88	3.14	4383600.0	4
	−542.6		−10.75	4487420.0	
SIRGAS2000	2.0		0.17	3740860.0	
	4.1	0.00	−0.03	−4964290.0	0
	3.9		0.07	−1425420.0	
SIRGAS95	7.7		0.00	3135390.0	
	5.8	1.57	0.00	−5017670.0	9
	−13.8		−0.03	−2374440.0	
GDA94	−56.8		−29.88	−4052050.0	
	6.8	11.80	−25.43	4212840.0	30
	49.7		−25.04	−2545110.0	
ETRF2000	53.5		1.99	3661090.0	
	50.6	2.42	12.06	845230.0	6
	−83.0		−19.49	5136850.0	

with the receiver-satellite unit-direction vectors related as $\mathbf{u}^s_{r,R} = \mathbf{R}\mathbf{u}^s_{r,G}$.

Subtracting Δs times Eq. (20) from Eq. (19) gives

$$||\mathbf{x}^s_R - \tilde{\mathbf{x}}_{r,R}|| - \Delta s||\mathbf{x}^s_G - \mathbf{x}_{*,G}|| \approx ||\mathbf{x}^s_R - \mathbf{x}_{r,R}|| - \Delta s||\mathbf{x}^s_G - \mathbf{x}_{r,G}|| \tag{21}$$

The right-hand side we recognize as $\rho^s_{r,G}$ (see (5)). Thus to first order, we have

$$\rho^s_{r,G} = ||\mathbf{x}^s_R - \tilde{\mathbf{x}}_{r,R}|| - \Delta s||\mathbf{x}^s_G - \mathbf{x}_{*,G}|| \tag{22}$$

with the 2nd term on the right-hand side being the 'clock-correction'. Substitution of (17) and (22) into (6) gives

$$p^s_r = ||\mathbf{x}^s_R - \tilde{\mathbf{x}}_{r,R}|| + cdt_r - c\widetilde{dt}^s_R + a^s_r + e^s_r \tag{23}$$

This result shows that with the 'clock-correction' approach one is actually solving for $\tilde{\mathbf{x}}_{r,R}$. Comparing (13) with (18) shows that $\tilde{\mathbf{x}}_{r,R} = \mathbf{x}_{r,R''}$ and that in case of the transformed clock, to first order, one is actually solving for the same position as in de scale-absorbed approach. Hence, the 'transformed-clock' (tc) bias is approximated by

$$\mathbf{b}^{tc}_r \approx \tilde{\mathbf{x}}_{r,R} - \mathbf{x}_{r,R} = -\Delta s\mathbf{R}(\mathbf{x}_{r,G} - \mathbf{x}_{*,G}) = \mathbf{b}^{sc}_r \tag{24}$$

which is identical to the scale-absorbed bias.

4.4 Numerical Values of the Scale Induced Bias

From the previous sections two equations for the remaining scale induced bias are available. For the unscaled approach this is Eq. (11) and for both the scale-absorbed and transformed clock approach this is Eq. (16). Both equations show that if $\Delta s = 0$, i.e. if GRF and RRF have identical scale, then there is no positioning bias. As Δs is time dependent, so is the scale induced bias. Table 1 gives the transformation parameters to generate the RBCs for August 9th 2013, this is the date for which the experimental results in Sect. 5 have been generated. The last column of Table 1 gives the maximum predicted remaining scale induced bias for the transformed clock RBC. For SIRGAS2000 there should be no scale induced bias as $\Delta s = 0$. The remaining scale induced bias for the transformed clocks approach, according to Eq. (16), increases with the distance from the reference point $\mathbf{x}_{*,G}$. For NAD83, ETRF2000 and SIRGAS95 the bias is less than 10 mm. For GDA94 the bias is up to 30 mm on the mainland of Australia, due to the large scale factor of GDA94 compared to the other RRFs. This resulting scale induced bias is significantly less than the scale induced bias resulting from the RBC of 75 mm using only the GRF-to-RRF transformation and no transformed clock (Huisman et al. 2012). The maximum predicted remaining scale induced bias is one magnitude smaller than the decimetre level precision that can be achieved with real-time PPP (e.g. BKG 2013b), but is significant in post-processing applications where millimetre level precision is achieved (Kouba 2009).

5 Experimental Results with Transformed Clocks

For each of the RBCs one station in the region has been processed for August 9th 2013, a list of processed stations is given in Table 2. The RBCs available from regional NTRIP-

Table 2 Regional reference frame and location information for processed stations

Station	RRF	Latitude	Longitude	Height (m)
azu1	NAD83	34.1°N	117.9°W	135
braz	SIRGAS2000	15.9°S	47.9°W	28
conz	SIRGSA95	32.0°S	73.0°W	186
cut0	GDA94	32.0°S	115.9°E	28.5
dlf1	ETRF2000	52.0°N	4.4°E	67

Table 3 Predicted bias approach, mean bias using the (Eq. (16)) for the RBCs generated RBC in PPP and their differences with the transformed clocks

Station	Component	Predicted Bias (mm)	Mean Bias (mm)	Difference (mm)
azu1	North	−1.1	−2.0	−0.8
	East	−1.0	−1.0	−0.1
	Up	+0.2	+1.3	+1.1
	Total	+1.5	+2.6	+1.1
braz	North	−0.0	+0.1	+0.1
	East	−0.0	+0.1	+0.1
	Up	−0.0	+0.0	+0.0
	Total	+0.0	+0.1	+0.1
conz	North	+2.4	+2.3	−0.0
	East	+2.4	+2.4	+0.0
	Up	−0.6	−0.7	−0.1
	Total	+3.4	+3.4	+0.0
cut0	North	+9.1	+9.5	+0.4
	East	+21.4	+22.0	+0.6
	Up	−3.7	−5.0	−1.4
	Total	+23.5	+24.5	+1.0
dlf1	North	+0.6	+0.9	+0.3
	East	+1.3	+1.5	+0.2
	Up	−0.6	−0.0	+0.5
	Total	+1.6	+1.7	+0.2

casters are generated using a combination of GBCs, however the corresponding combined GBC is not available, which makes it impossible to compare results. Therefore RBCs have been generated with the BNC version 2.9 software using the IGS01 GBC as input. Besides generation of the RBCs also a GBC has been created using BNC 2.9, such that GBC and RBCs used in the data processing have the same sampling rate. BNC 2.9 has also been used to compute PPP solutions using the GBC and relevant RBC for each station. Table 3 and Fig. 1 summarize the remaining bias for the transformed clocks RBCs. The table shows for each station the predicted bias, given by the scale absorbed bias from Eq. (16), and the bias from the PPP processing. The figure gives the times series of the bias for station CUT0 in Perth, Australia. In all cases the bias is computed as $x_{r,RBC} - x_{r,GBC}$, where $x_{r,RBC}$ is the position obtained using the

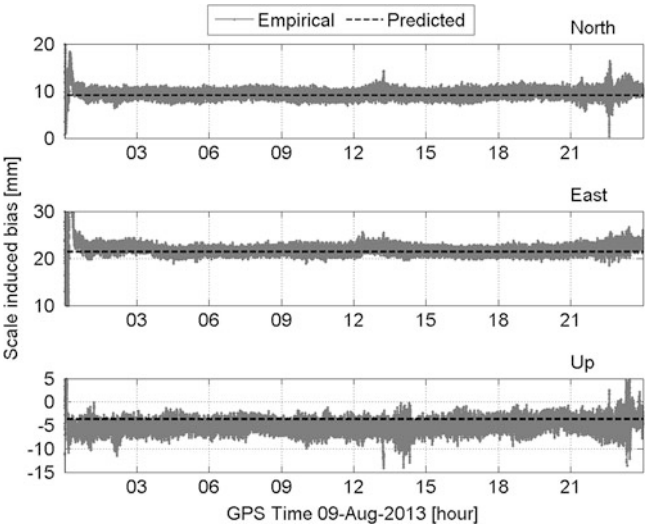

Fig. 1 Remaining scale induced bias using the transformed clocks RBCs at August 9th 2013, for station CUT0, Perth, Australia. *Gray line* gives the empirical bias from PPP processing, the *black dotted line* shows the predicted bias from (16)

RBC and $x_{r,GBC}$ is the position obtained from the GBC and then transformed to the RRF. The mean difference between the empirical bias from processing and the predicted bias is close to or less than 1 mm for all stations. The results show that the scale absorbed bias gives a good prediction for the transformed clock bias. As can be seen from Fig. 1, the transformed clock bias does not vary a lot with the 1 Hz observation rate of this dataset.

6 Conclusions

Using the 14-parameter transformation on the server side to generate RBCs causes scale induced biases in the PPP positions. Three methods have been given to deal with the scale induced bias, the unscaled, the scale-absorbed and the transformed clocks approach. For all three methods there are remaining residual scale induced biases. The bias for the unscaled and scale-absorbed approaches scan be computed / predicted exactly. This contribution has shown that the remaining bias in the transformed clocks approach can be approximated very well with the bias for the scale-absorbed approach. Using currently available RBCs causes scale induced biases of less than 10 mm in the case of ETRF2000, NAD83 and SIRGAS95. For SIRGAS2000 there is no scale induced bias, since in the generation of this RBC there is no increment to the scale factor. For GDA94 the remaining scale induced bias is maximum 30 mm, which is caused by the large scale factor of GDA94 compared to other RRFs.

Acknowledgements The second author is the recipient of an Australian Research Council (ARC) Federation Fellowship (project number FF0883188). Part of this work was done in the framework of the project 'New Carrier-Phase Processing Strategies for Next Generation GNSS Positioning' of the Cooperative Research Centre for Spatial Information (CRC-SI2).

References

BKG (2013a). http://igs.bkg.bund.de/ntrip/orbits

BKG (2013b). ftp://igs.bkg.bund.de/NTRIP/ppp/performance.13-08-09

Caissy M, Agrotis L, Weber G, Hernandez-Pajares M, Hugentobler H (2012) Innovation-coming soon-the international gnss real-time service. GPS World 23(6):52

Hauschild A, Montenbruck O (2009) Kalman-filter-based GPS clock estimation for near real-time positioning. GPS Solutions 13(3):173–182

Huisman L, Teunissen PJG, Hu C (2012) GNSS precise point positioning in regional reference frames using real-time broadcast corrections. J Appl Geod 6(1):15–23

IGS.org (2013) Real-time service. http://rts.igs.org/

Kouba J (2002) The GPS toolbox ITRF transformations. GPS Solutions 5:88–90. doi:10.1007/PL00012903. http://dx.doi.org/10.1007/PL00012903.

Kouba J (2009) A guide to using International GPS Service (IGS) products. Publication of the IGS Central Bureau, Online at http://igscb.jpl.nasa.gov/igscb/resource/pubs/UsingIGSProductsVer21.pdf

Rebischung P, Griffiths J, Ray J, Schmid R, Collilieux X, Garayt B (2012) IGS08: the IGS realization of ITRF2008. GPS Solutions 16(4):483–494. doi:10.1007/s10291-011-0248-2. http://dx.doi.org/10.1007/s10291-011-0248-2

RTCM (2011) RTCM-10410.1 Standard for Networked Transport of RTCM via Internet Protocol (Ntrip), Version 2.0 with Amendment 1, June 28, 2011

Takasu T (2010) Real-time PPP with RTKLIB and IGS real-time satellite orbit and clock. In: IGS Workshop

Teunissen PJG, Huisman L, Hu C (2012) Real-time precise point positioning in NAD83: global and regional broadcast corrections compared. J Surv Eng 139(1):1–10

Weber G (2013) BKG Ntrip Client (BNC) Version 2.9 – Manual. Federal Agency for Cartography and Geodesy (BKG). Frankfurt, Gemany

Weber G, Dettmering D, Gebhard H, Kalafus R (2005) Networked transport of RTCM via internet protocol (Ntrip)-IP-streaming for real-time GNSS applications. In: ION GNSS 18th International Technical Meeting of the Satellite Division, pp 13–16